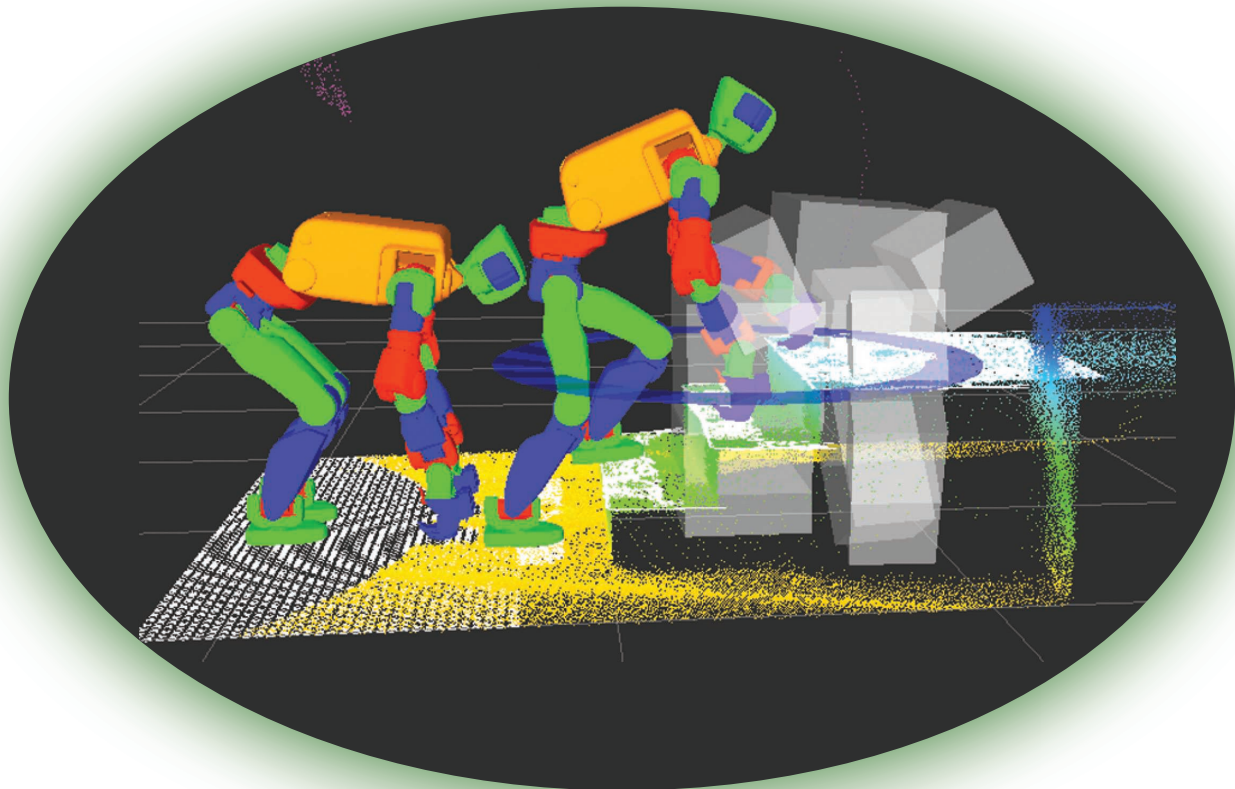


By Takahide Yoshiike, Mitsuhide Kuroda, Ryuma Ujino, Yoshiki Kanemoto, Hiroyuki Kaneko, Hirofumi Higuchi, Satoshi Komuro, Shingo Iwasaki, Minami Asatani, and Takeshi Koshiishi



The Experimental Humanoid Robot E2-DR

A Design for Inspection and Disaster Response in Industrial Environments

Against the backdrop of a rising number of disasters in industrial facilities due to a lack of maintenance, robots are expected to increasingly undertake dangerous, dirty, and laborious tasks conventionally performed by humans, such as daily maintenance and inspection of industrial plants. It is much safer to use robots to gather information

and conduct first response, but, with the installation of new equipment over time, the narrow premises of industrial infrastructure become obstructed with equipment. Robots navigating these spaces must achieve mobility utilizing narrow pathways, steep stairs, vertical ladders, and gaps while also fulfilling manipulation tasks like opening doors and valves.

This article presents E2-DR, an experimental humanoid robot for disaster response. We provide details on the software, electronics, and operational procedure as well

Digital Object Identifier 10.1109/MRA.2019.2941241

Date of current version: 21 October 2019

as experiments for standing up, absorbing impact, and handling collisions while walking. Accompanying video of the experiments are available for online viewing.

Robots Navigating Confined Spaces

Crawler-type and quadruped robots, such as those in [1] and [2], face a variety of challenges in industrial environments. They cannot climb vertical ladders and may have difficulty mounting steep stairs and rotating in such narrow spaces as stair landings. Considering that industrial facilities are designed and maintained so humans may navigate and work efficiently, humanoid robots are a promising alternative, as demonstrated in the DARPA Robotics Challenge. However, conventional humanoid robots like JAXON [3], DRC-Hubo [4], and RoboSimian [5] have not yet reached the required level of mobility in complicated and narrow environments.

Robots sometimes have to deal with unexpected collisions caused by misoperation, the uncertainty of external sensors, or slippery surfaces. Although autonomous collision detection [6] can help reduce the risk of falling down, large external forces are to be expected. To absorb the impact during these unexpected collisions, whole-body joint torque control is one possible option. Robots with torque-controlled joints are able to react to external forces. However, implementing a whole-body torque-control system in a slim humanoid robot is still a big challenge. Torque-controlled legged robots like Valkyrie [7] and WALK-MAN [8] are too large and heavy to move in complicated and narrow environments. Both are more than 1,850 mm tall and weigh over 120 kg.

We previously reported a new experimental humanoid robot, E2-DR (Experimental robot type 2 for Disaster Response) [9], [10], which can work in confined environments with the ability to handle unexpected collisions, as shown in Figure 1. In [9], we introduced a new approach for dust- and splashproofing and presented experiments like climbing a vertical ladder and walking on scattered debris. In [10], we reported details of the torque-control actuator and additional experiments using the torque controller.

Operating in Disaster-Stricken Plants

The primary goal of our robot is inspection and maintenance in industrial environments, such as plants. Therefore, we focus on such scenarios as a small explosion in a manufacturing facility, with scattered debris but where the structural integrity is maintained. Here, robots may proactively act as first responders by manipulating valves or switches to prevent further destruction.

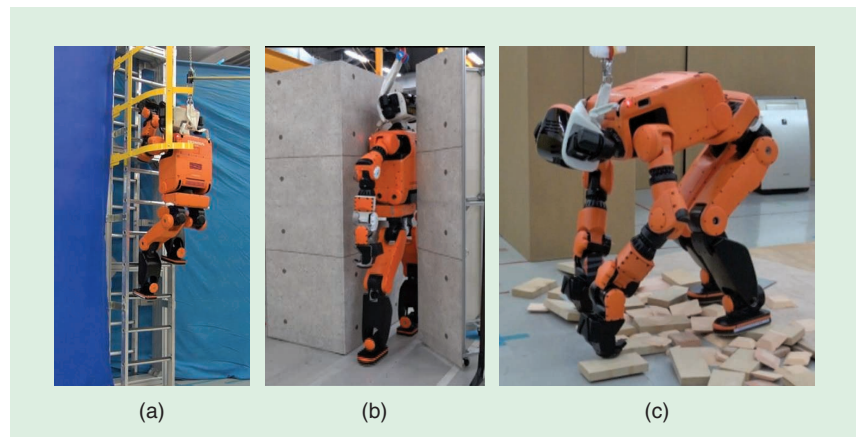


Figure 1. The experimental humanoid robot E2-DR (a) climbing a vertical ladder with a fall-prevention cage, (b) walking through a 300-mm narrow space, and (c) walking on scattered debris.

Functional Requirements

To navigate a typical plant, the robot must be able to

- move up and down 3D structures
- move along narrow pathways and in narrow spaces
- move on scattered debris
- absorb impacts while moving.

Concerning manipulation, specialized tools with remote-control features are available. Thus, the proposed robot does not need dexterous hands but only the ability to grasp tools and structures, such as the rung of a ladder to move.

Environmental Requirements

We investigated oil refineries and power generation plants and surveyed standards, such as International Organization for Standardization (ISO) 14122-1, to define the dimensions of the target environments. The specifications of stairs, step ladders, and vertical ladders are shown in Table 1, as a robot would have to climb up and down vertical ladders with narrow fall-prevention cages. The minimum width of a pathway is defined as 600 mm in ISO 14122-2. There is an exception when the pathway may be reduced to no less than 500 mm for a short distance if the working pathway is used only occasionally. In our

Table 1. The environmental requirements of stairs (measured in millimeters).

	Stairs	Step Ladders	Vertical Ladders	
Height	<265	200–340	Distance between rungs	225–350
Depth	>200	>80	Width	320–600
Width	>520	>450	Diameter of rungs	20–40
Height of handrail	900–1,000		Diameter of fall-prevention cage	650–800

investigation of actual plants, there are spaces with 300-mm widths used in the event of an emergency.

Dust- and splashproofing is required for usage in rainy outdoor fields or under broken pipes. We concluded that the robot should be compliant with the Ingress Protection 53—defined in International Electrotechnical Commission standard 60529—dust- and splashproofing standards.

Overview of E2-DR

Hardware Design Considerations

For locomotion in a narrow environment, biped walking is more advantageous than quadruped movement because the projected area of the robot to the ground is smaller. On the other hand, for locomotion over scattered debris, quadruped walking is better in terms of robustness because of the wider projected area. Therefore, E2-DR has the ability to move forward selectively with biped or quadruped walking based on the environmental situation [11]. This schema was also realized by Kojima et al [3].

RoboSimian [5] adopted a general-purpose design for all of its limbs. In this approach, a limb may be repurposed for recovery if another limb is broken. However, unifying the design of the limbs for bipedal walking and manipulation tasks increases the weight and size of the robot. Therefore,

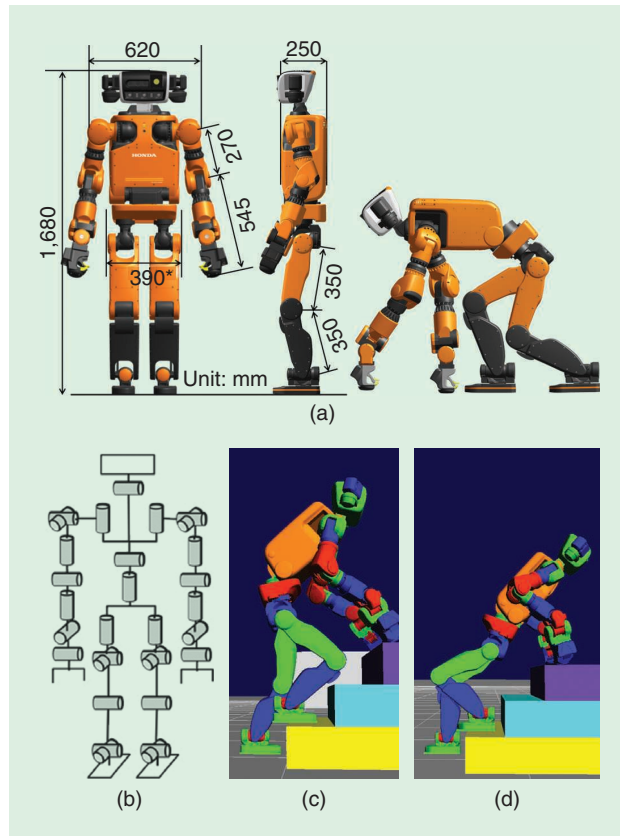


Figure 2. The E2-DR's (a) dimensions, (b) DoF, (c) knee configuration while climbing up steps as a quadruped, and (d) reverse knee configuration while climbing steps quadrupedally. Compared with (c), the risk of collision at the shin is lower.

we adopted a specialized approach for designing the arms and legs.

To realize quadruped walking, the robot's end effector supports the robot's weight as it walks on its knuckles. To mitigate the risk of toppling from high places if the robot unexpectedly shuts down, the end effectors are equipped with a nonexcitation actuating brake between the motor and harmonic drive gear to maintain their grasp.

E2-DR Specifications

The height of the robot is 1,680 mm, and the total weight is 85 kg, including a 1,000-Wh lithium-ion battery in the torso,

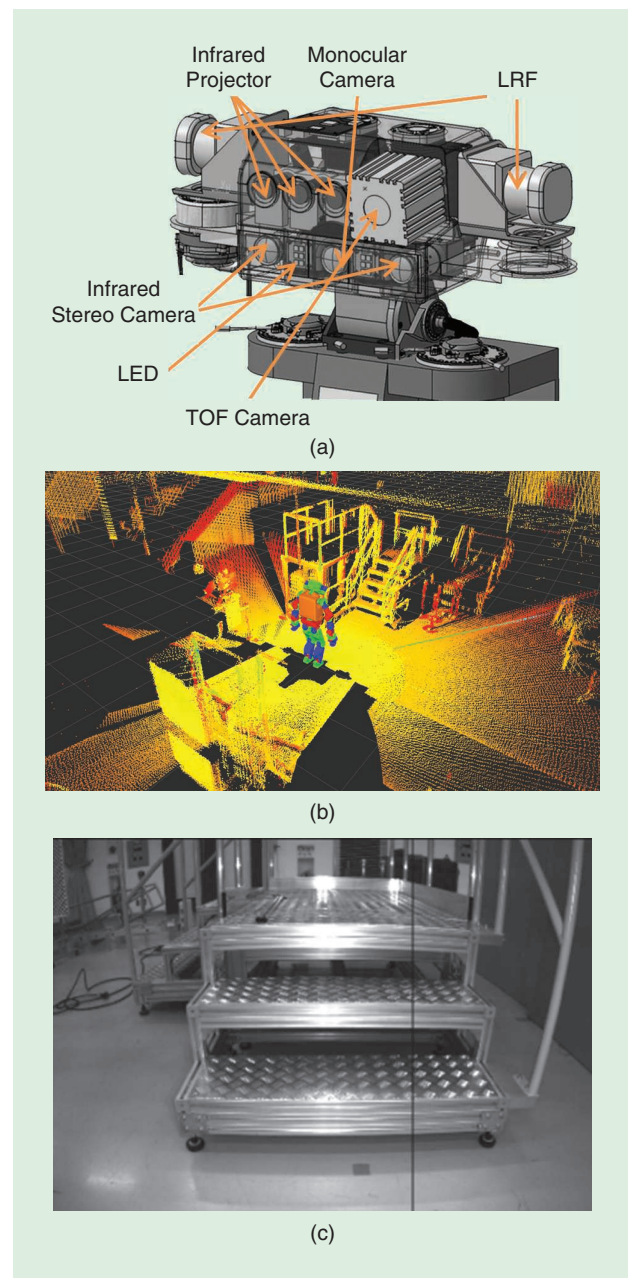


Figure 3. (a) The sensors mounted on E2-DR's head. (b) The point cloud data acquired by the LRFs. (c) The output image of the monocular camera on the head. TOF: time of flight.

which provides 90 min of operating time. One of the major features of the robot is its thickness, being just 250 mm at its thickest point.

The robot has a total of 33 degrees of freedom (DoF), as shown in Figure 2. At the base of the torso, a high-torque pitch joint with a wide range of motion enables transitioning between biped and quadruped walking. A yaw joint enables the upper body to rotate 180°. This joint, in particular, enables switching from knee configuration [Figure 2(c)] to reverse knee configuration [Figure 2(d)]. Reverse knee configuration is useful in preventing collisions between the robot's shins and stairs.

Sensors Mounted on E2-DR

Sensors are installed on the head by considering the fields of view in biped and quadruped walking, as shown in Figure 3(a). Two laser range finders (LRFs), Hokuyo UTM-30LX-EW, are located at the same positions as a human's ears. By rotating them along the yaw axis, the robot can obtain 360° point cloud data, as shown in Figure 3(b). Point cloud data are not affected during a

blackout, so the operation of the robot is mainly done with point cloud data from LRFs. The robot also has a monocular camera [indicated in Figure 3(c)] to show images to the operator. It is equipped with a synchronized electronic flash employing LED for use during blackouts. Images are used only in limited applications, such as reading equipment meters. Therefore, the robot has only a single DoF for the head due to the LRFs' 360° capabilities. Additionally, the robot has an infrared-light-projected stereo system and a time-of-flight camera on its head for real-time walking on uneven floors.

Table 2. The specifications of the torque sensors.

	Hip Roll	Knee Pitch	Upper Arm Twist
Peak torque (Nm)	180	280	95
Stiffness (Nm/rad)	29,000	57,000	29,000

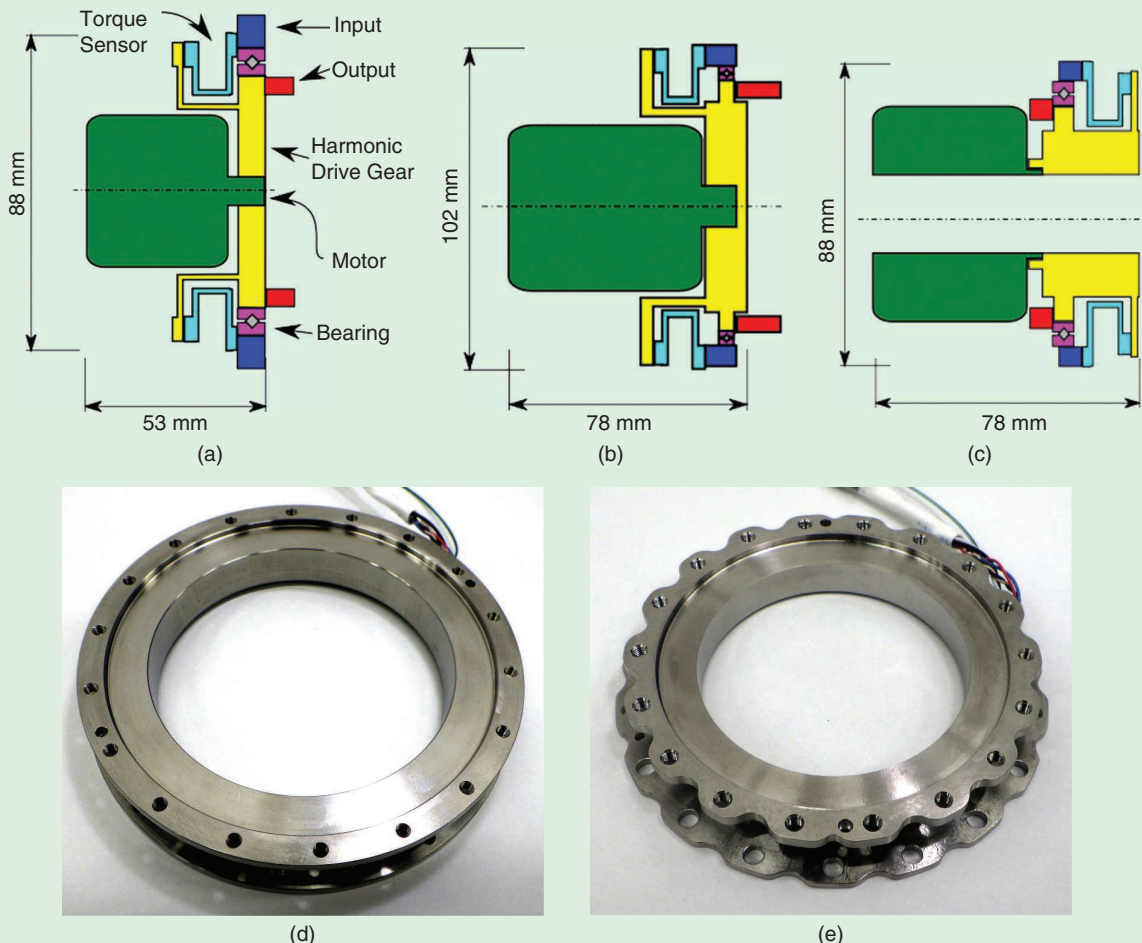


Figure 4. The mechanical layout of the proposed actuators: the (a) hip roll, (b) knee pitch, and (c) upper arm twist. (d) The shape of the torque sensor of the knee pitch joint. (e) The shape of the torque sensor of the hip roll and upper arm twist joints.

Joint Torque Control

It is desirable to have a torque-control system with high bandwidth and low tracking error to produce extremely

Crawler-type and quadruped robots cannot climb vertical ladders and may have difficulty mounting steep stairs.

relatively large deflection to ensure sufficient torque-sensing resolution. Thus, we employed a system based on strain

compliant behavior and precise movement. However, actuators with torque sensors must be compact for robots to work in narrow environments. It is possible to use an encoder [12] as a spring deflection sensor to enable joint torque control. However, these have a limitation because they require a relatively large deflection to ensure sufficient torque-sensing resolution. Thus, we employed a system based on strain

gauges attached to flexure elements [13]. They are thin films, have sufficient sensitivity, and are attached to relatively stiff sensors [14].

The actuator unit consists of a brushless dc motor, harmonic drive gear, and torque sensor. The design of our torque-controlled actuator is characterized by a ring-shaped torque sensor placed outside of the motor or the gear [10]. This layout shortens the axial length of the actuators. Figure 4 shows the structures of some joints. Our sensors are designed to have a thin, cylindrical flexure part with strain gauges attached and flanges to connect gears and links, as shown in Figure 4(d) and (e). The thickness of the flexure part is determined as 0.15–0.2 mm to maximize the resolution while satisfying the strength requirements. Table 2 shows the specifications of the designed torque sensors.

A proportional-derivative controller with a disturbance observer for the torque-control system is chosen because of its ease of tuning and its robustness. The time constant of the feedback control is 1.5 ms. A Bode plot of the torque-tracking performance is shown in Figure 5. Consequently, a control bandwidth of over 100 Hz is achieved. The robot was hanging above the ground during these measurements, so the joint loads were not fixed.

System Overview

E2-DR is equipped with an electronic control unit (ECU) for managing its motions (the motion-control ECU), with an Intel Core i7 2.4-GHz CPU. There is also an ECU for perception and recognition (the recognition ECU), with an Intel Core i7 2.2-GHz CPU and a Haswell graphics processing unit. In addition, the robot is equipped with distributed motor control ECUs and drivers for driving motors, joint torque sensors, and six-axis force torque sensors attached on its wrists and ankles, as shown in Figure 6. The motion-control ECU communicates with those devices through its internal network, with a sampling rate of 1 kHz. The robot is remotely teleoperated by communicating with a console PC operated via a wireless local area network.

To reduce the risk of cables disconnecting because of a high harness occupancy rate, we use 0.5-mm-diameter optical fiber for internal network communication. The major concern for optical fiber when used in a robot's joints is mechanical tolerance and attenuation during twisting and bending. After performing cycle endurance tests of twisting and bending optical fiber 1 million times, it was concluded that the cable meets the tolerance and attenuation requirements.

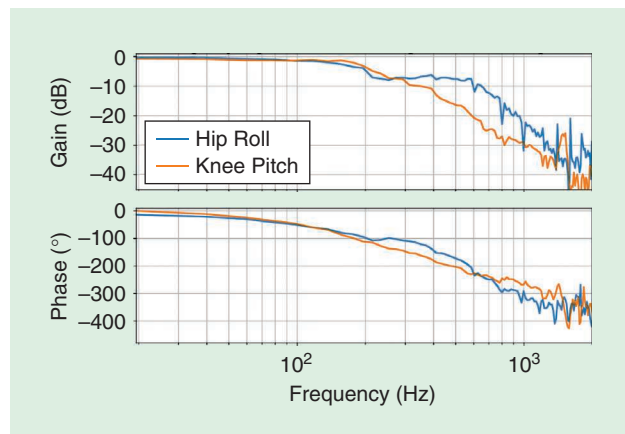


Figure 5. A Bode diagram of the closed-loop torque tracking for the hip roll and knee pitch joints, showing the frequency response from the desired torque to the measured torque.

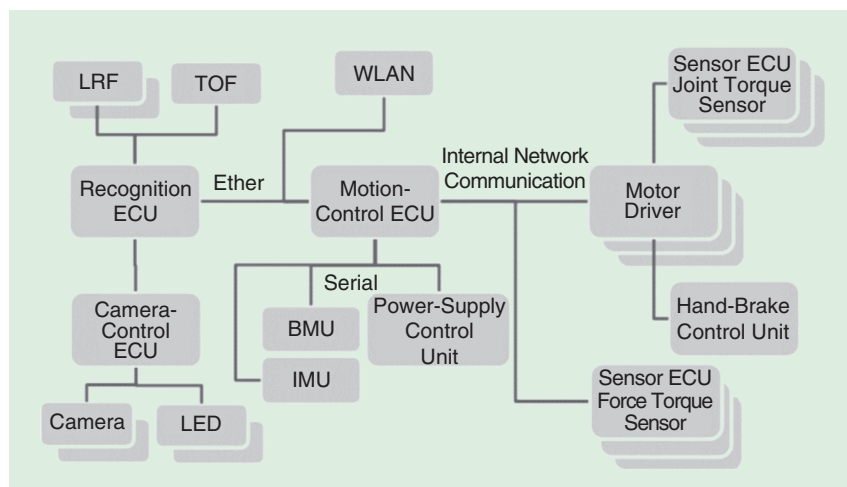


Figure 6. The electrical system and internal network configuration of E2-DR. WLAN: wireless local area network; IMU: inertial measurement units; BMU: battery management unit.

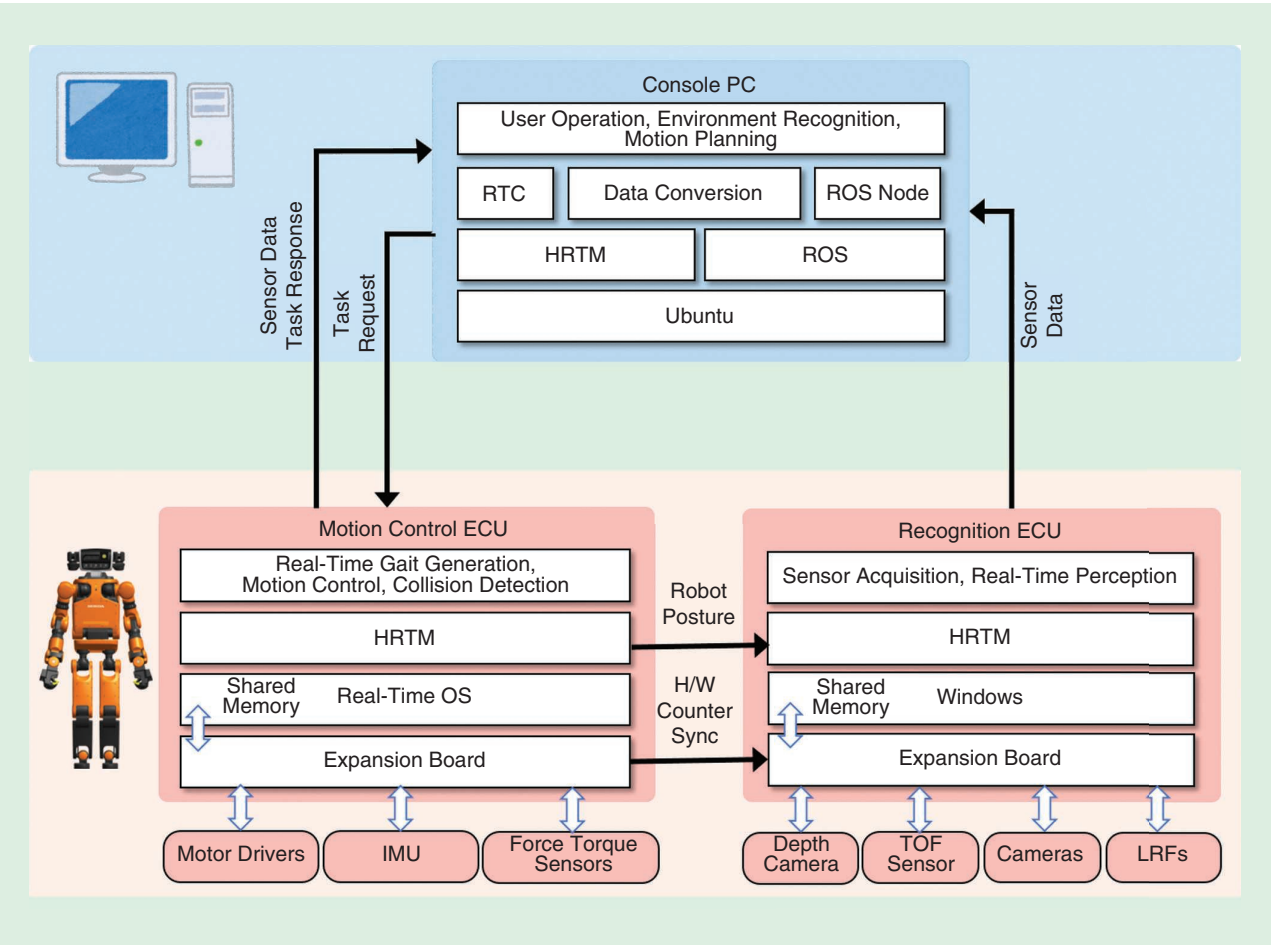


Figure 7. The software architecture of the E2-DR. RTC: robotic technology component.

Software Overview

The robot is remotely teleoperated, but it also behaves semi-autonomously in perception, motion generation, and motion control under the instruction of the operator. The software architecture of E2-DR is designed as shown in Figure 7.

As the motion-control ECU runs at a 1-kHz sampling rate, it tracks reference motion while maintaining the desired center of mass (CoM) and outputs motor commands to the motor drivers. Honda RT-Middleware (HRTM) [15] was used as middleware, which is a real-time extension of RTM by Object Management Group. VxWorks, a real-time operating system (OS), was used as the OS.

On the recognition ECU, data from sensors, such as 3D measurements by the LRFs and cameras, are transferred to the console PC. Windows is used as its OS because some device drivers are supported only on Windows. Real-time perception functions like the evaluation of floor surfaces for locomotion will be implemented here in the future.

An external console PC serves as the interface for the operator. Additionally, environment recognition and motion planning are done here. The motion planning

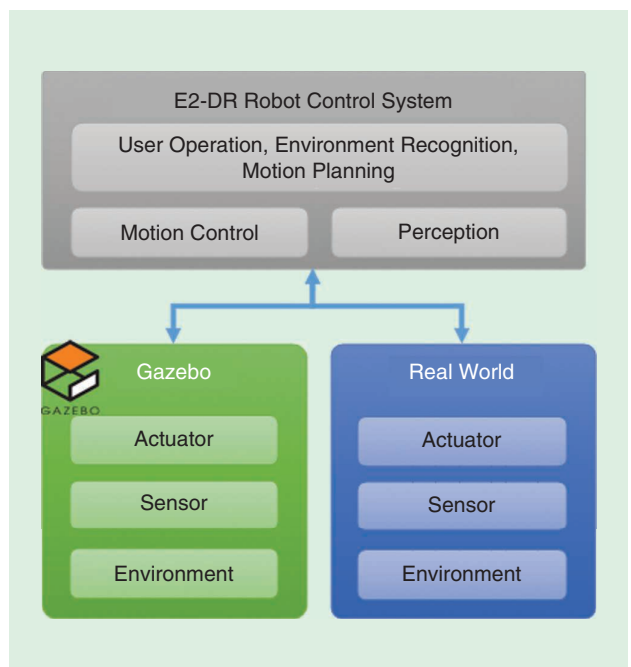


Figure 8. The E2-DR software architecture can also be connected to the Gazebo simulator as well as to robots in the real world.

function generates the reference motion of the robot in time series. Robot Operating System (ROS) is used as the middleware for the interface and environment recognition because of its ease to implement functions. Consequently, Rviz is adopted as the graphical user interface. To connect the two types of middleware, a data conversion interface, HRTM-ROS bridge, was developed. The software architecture can also be connected to the Gazebo simulator, as shown in Figure 8.

Robots may proactively act as first responders by manipulating valves or switches to prevent further destruction.

connected to the Gazebo simulator, as shown in Figure 8.

Teleoperation Procedure Overview

Teleoperation consists of five steps: user operation, recognition of environment, motion planning, confirmation by the operator, and motion control.

User Operation

A user gives instructions by selecting a type of motion, such as bipedal, quadrupedal, or door passing and destination. Meanwhile, the robot is capable of autonomously generating its trajectory without colliding with the surrounding environment, including its landing-positions-based 3D point cloud data. Figure 9 shows an example of the instructions an operator has provided.

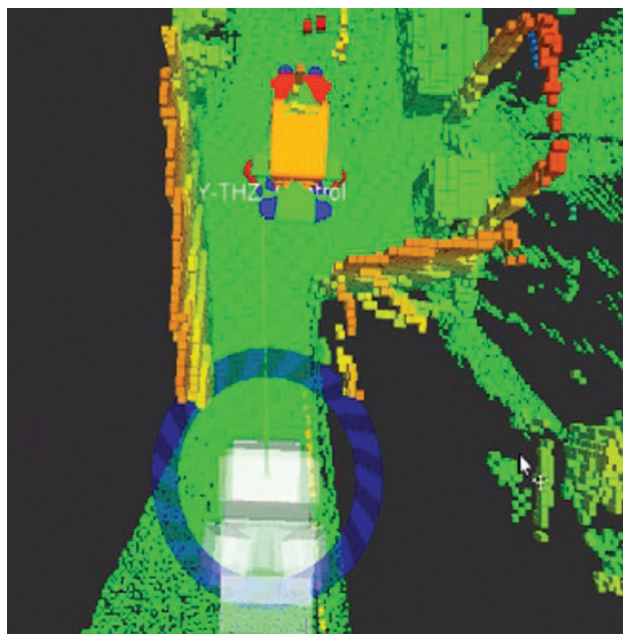


Figure 9. The operation of passing through a narrow pathway. A person can operate the robot by just providing the target position and orientations, with the blue circle in the voxel grid calculated from point cloud data. The white transparent robot shape in the blue circle is the approximate target position of the robot.

Recognition of the Environment

The robot autonomously recognizes its surrounding environment using knowledge on structures like stairs, ladders, and door knobs. The separation of the target region from its surrounding environment is done by a user through a simplified interface. Recognition of a ladder is accomplished using point cloud data acquired through the LRFs [Figure 10(a)]. First, a ladder structure is clipped through floor surface recognition. Next, the side rails of the ladder are cut out by extracting a circular cylindrical shape in the vertical direction by the random sample consensus method, including smoothing with the moving least-squares technique. The remaining rungs are recognized as cylindrical shapes using the same approach. After proper sensor calibration, relatively high precision was empirically verified, as shown in Figure 10(b). The recognition of the ladder can be completed in seconds, and it does not significantly affect the teleoperation of the robot from the operator's perspective.

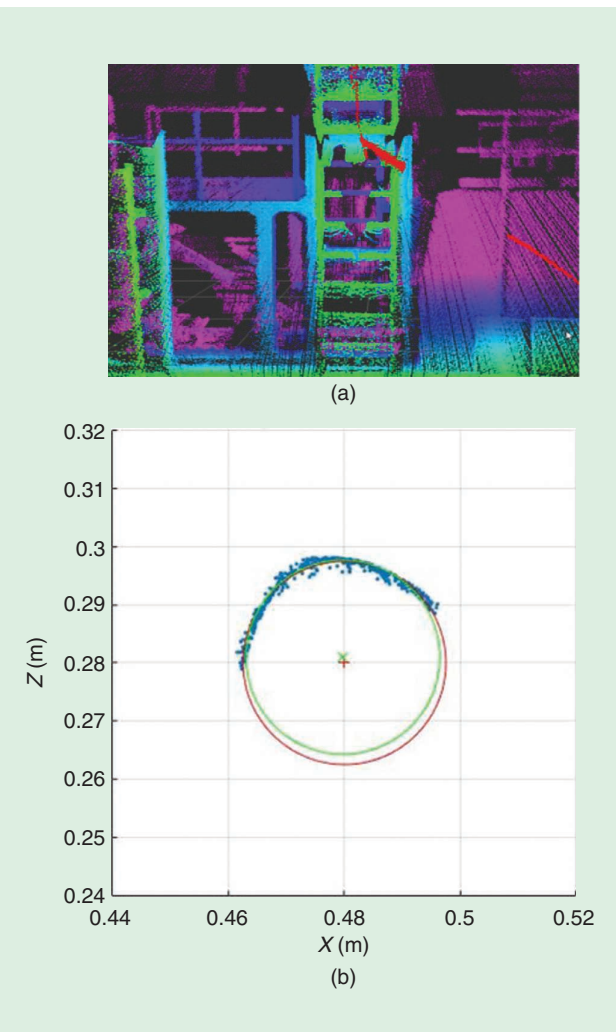


Figure 10. Model-based recognition of the environment: (a) the measured point cloud data of a ladder; (b) the matching of a rung, with smoothing by the moving least-square method.

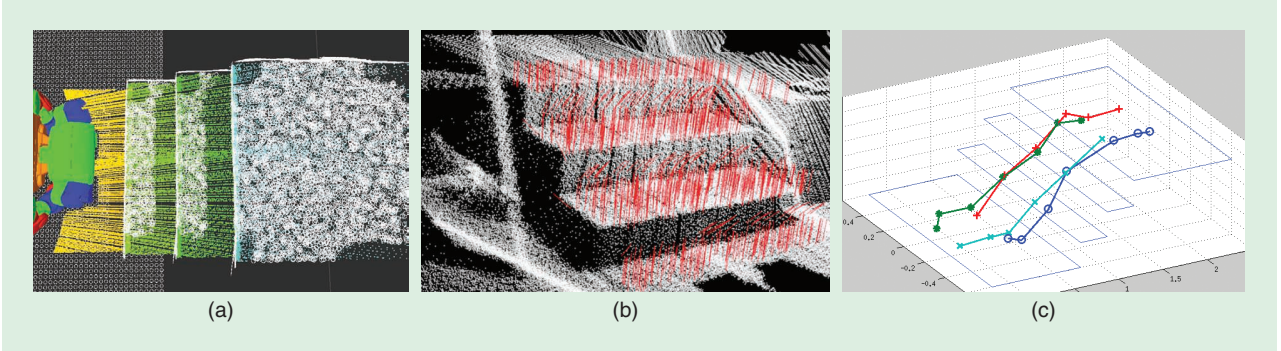


Figure 11. (a) Candidates for landing positions (white areas). (b) The calculation of the normal direction. (c) An optimal sequence of landing positions to climb up stairs in quadruped fashion. The blue and light blue points show the sequences of the landing positions of the right hand and right foot. The red and green points show those of the left hand and left foot.

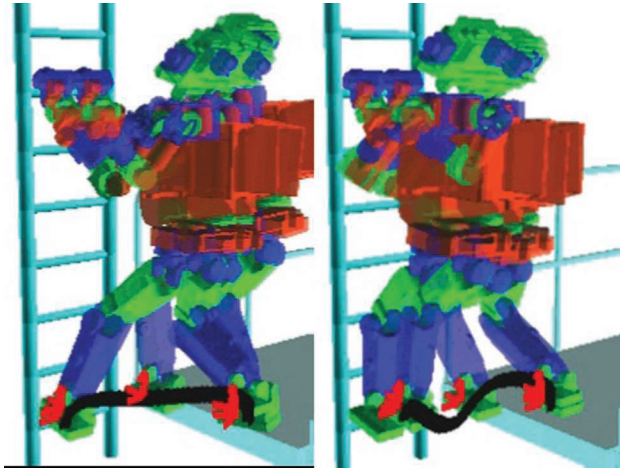


Figure 12. An example of a generated key pose. The red points are the key frame end effector's trajectory, and the black points are the end effector's trajectory. We set the number of key frame divisions to 10 (the figure shows the key frames separated into three intervals for visibility).

Motion Planning

For motion planning, a sequence of reference motions is generated by the robot online, based on recognition of the environment. The reference motions should be checked in advance to reduce the risk of misoperation. However, a real-time gait planner on the robot has been implemented for high-speed walking in open environments, where commands are supplied via a joystick interface.

We have prepared two types of motion planners: the gait planner [11] and whole-body motion planner [16]. The former is mainly intended for locomotion on floors. The latter is meant for movements in such 3D environments as ladders. These planners are selected depending on the task.

The gait planner can deal with dynamic transition between biped and quadruped walking. Dynamic transition enables a robot to walk stably in quadruped fashion and temporarily in the biped manner when encountering a large gap that the robot cannot step over in the quadruped configuration because of kinematic constraints. In the gait planner, the landing positions of the robot can be

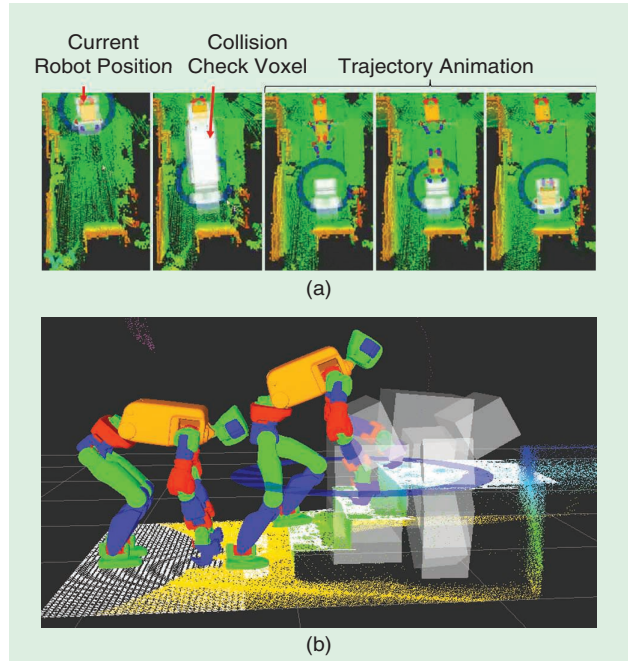


Figure 13. An example of confirmation by the operator. (a) The operator can check collisions of the robot with the environment throughout the entire trajectory using animation in the voxel grid calculated from point cloud data. In between the target position (blue circle) and the initial position, the system shows a snapshot of the robot along the trajectory. (b) The operator also can check three-dimensional movements, such as climbing stairs, with animation.

automatically determined according to the surface shape of the measured floors. Here, a sequence of landing positions is determined based on a combinatorial search from discretely scattered landing position candidates the size of the robot's foot, as shown in Figure 11(a). Inappropriate candidates, such as on steep slopes and the edges of steps, can be excluded by evaluating the normal directions [Figure 11(b)] and the level of flatness of the candidate region. A resulting optimal sequence of landing positions to climb up stairs quadrupedally is shown in Figure 11(c).

The whole-body motion planner needs to satisfy various constraints, such as balance, contacts, joint limitations,



Figure 14. (a) Bipedal walking at 4 km/h. (b) Quadrupedal locomotion at 2.3 km/h. (c) Stepping over a pipe 200 mm in diameter. (d) The transition from quadruped to biped.

kinematics, and collisions. We previously proposed a method for generating full-body trajectories based on key poses, considering these constraints at each key frame and then generating a full-body trajectory through instantaneous calculations considering the constraints [16] (see

Figure 12). These motions can be generated based on environmental models, such as intervals between the rungs of ladders reconfigured according to the measured data.

Confirmation by the Operator

To help the operator intuitively imagine the motions of the robot, the generated reference motions are shown through animation on a voxel grid representation calculated from the measured point cloud data, as shown in Figure 13(a) and (b). After checking it, the operator gives instructions to execute the motions. With this user interface, the risk of misoperation can be mitigated.

Motion Control

The motion controller tracks the reference motion while maintaining a desired CoM. Currently, two types of controllers are used: position based and torque based. One of these is selected depending on the experiment.

The position-based controller applies a feedback loop through reaction force control [17] to recover the robot from an inclination error while walking on the floor. The reaction force control modifies the desired zero moment point (ZMP) to recover the inclination error. To match the actual ZMP to the desired one, the position and

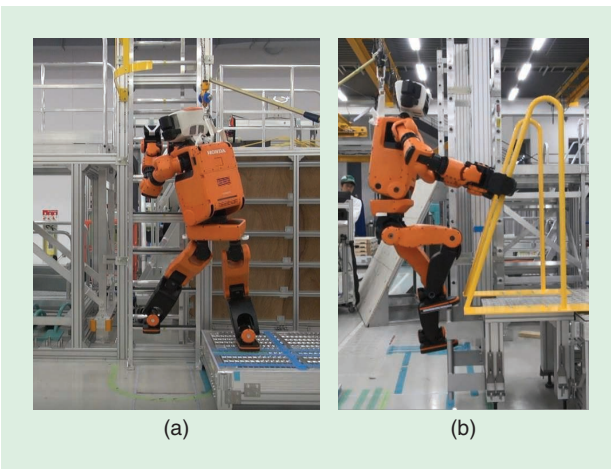


Figure 15. (a) A depiction of E2-DR's transition from ladder climbing to stepping sideways. (b) The transition from ladder climbing to stepping forward.

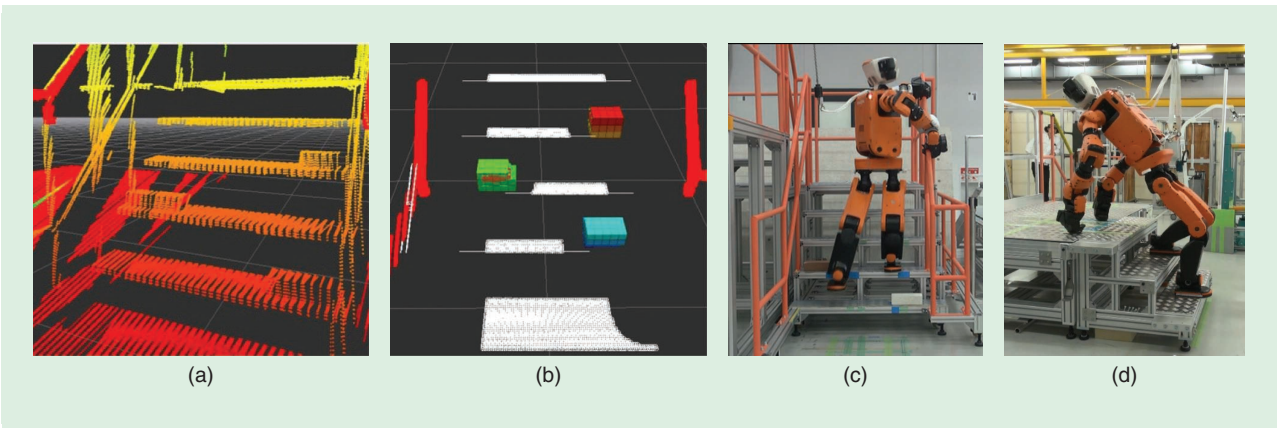


Figure 16. (a) The point cloud data of stairs with obstacles. (b) The recognized result of the obstacles and surface on the stairs where the robot can land its feet (white areas). (c) An experiment to climb stairs with obstacles while grasping a part of the environment. (d) Climbing stairs in the quadruped manner with reverse knee configuration.

orientation of the robot's feet are modified by force control. Then, all joint angles are calculated by inverse kinematics. When the robot climbs up vertical ladders, another controller [18] is adopted to recover the posture of the robot by modifying the landing positions according to the estimated amount of slippage.

The torque-based controller tracks reference whole-body motions. An inverse dynamics solver calculates the joint torques by solving the weighted minimization of errors between the desired and expected accelerations in the task space while satisfying centroidal dynamics and unilateral contact constraints [19].

Experiments With the Robot

Experiments to Show Functional Feasibilities

The following experiments were executed with a position-based controller because the experiments were set up so as not to have unexpected collisions.

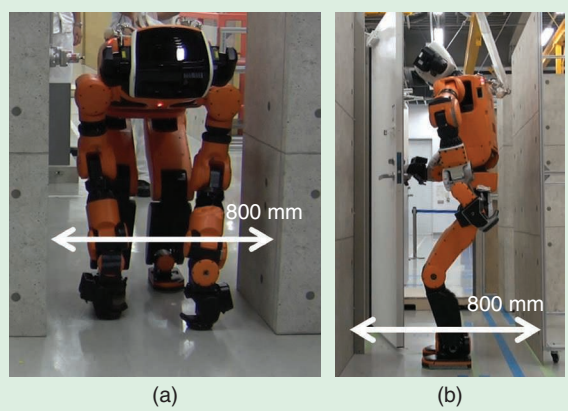


Figure 17. (a) Quadrupedal walking along an 800-mm-wide pathway. (b) Passing through a door to enter a room from a narrow corridor 800 mm in width.



Figure 18. E2-DR stepping over 100-mm-high steps piled with debris.

Basic Movement on a Floor

To evaluate basic walking ability, biped walking [Figure 14(a)] and quadruped walking [Figure 14(b)] were tested. The inclination error of the upper body in those experiments was under 1.5°. As one advantage of bipedal locomotion, walking over a pipe [Figure 14(c)] was tested. The transition between bipedal and quadrupedal movement was also tested [Figure 14(d)].

Vertical Movement: Ladder

Instances of vertical ladder climbing, with a narrow cage and transitions from ladder to steps, were tested [Figure 1(a) and Figure 15].

Vertical Movement: Stairs

An experiment for avoiding obstacles on stairs was conducted with the robot grasping handrails to prevent catastrophic falls, as shown in Figure 16. Quadruped walking on wider stairs without handrails was also realized, as shown in

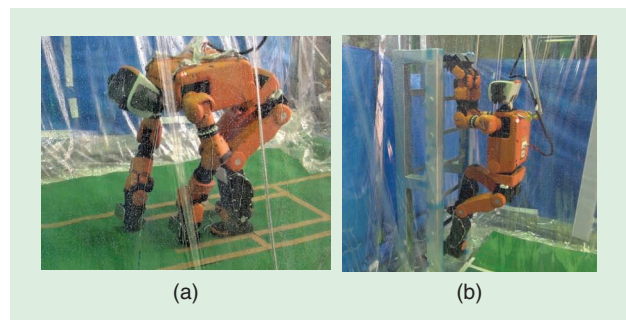


Figure 19. A splashproofing test: (a) quadruped walking under 26-mm/h rain and (b) ladder climbing under 26-mm/h rain.

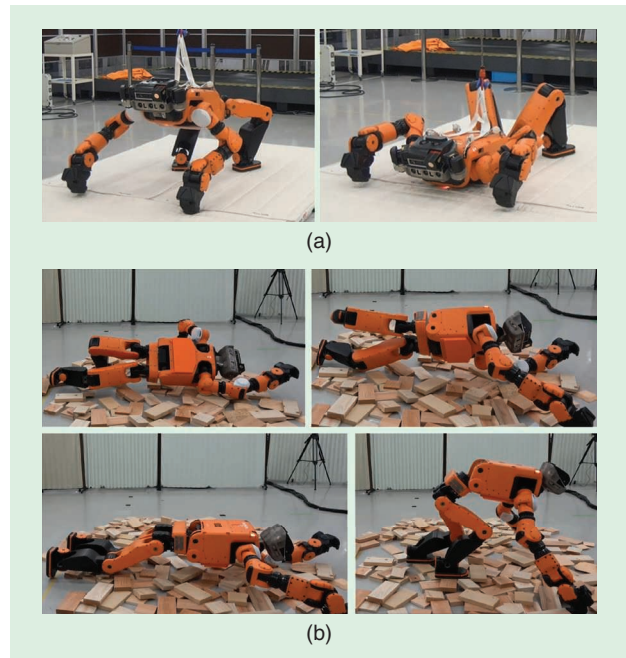


Figure 20. (a) E2-DR's transition to a waiting posture. (b) The robot standing up on debris after lying on its back.

Figure 16(d). The reverse knee configuration was used to prevent collisions between the robot's shins and the stairs for both experiments.

Movement in a Narrow Pathway and Narrow Space

Quadruped walking along an 800-mm pathway [Figure 17(a)] and biped locomotion through a 300-mm space [Figure 1(b)] were tested. Additionally, a demonstration of passing

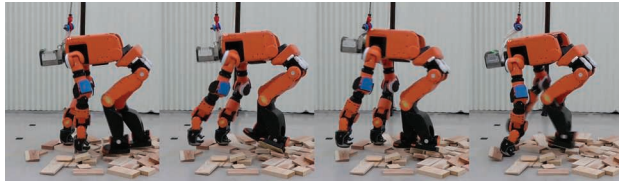


Figure 21. Slow walking at 0.72 km/h on scattered debris.

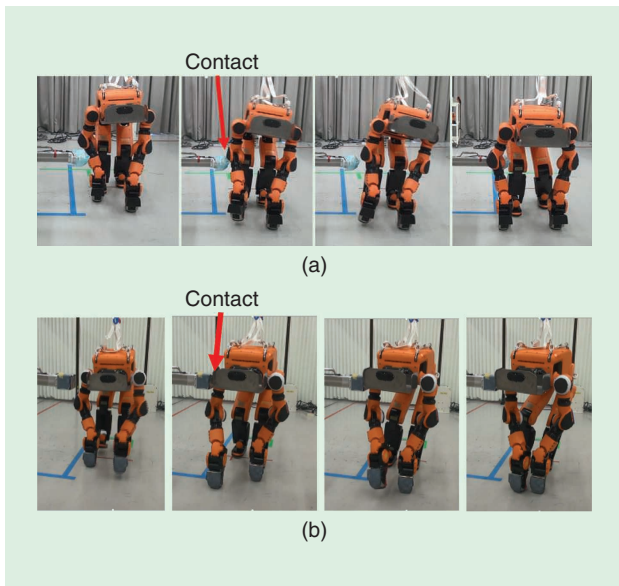


Figure 22. (a) The E2-DR's arm colliding while walking quadrupedally at 0.7 km/h. The right arm moved to absorb the force from the contact. (b) The robot hits its right shoulder, absorbing the impact using whole-body joint compliance.

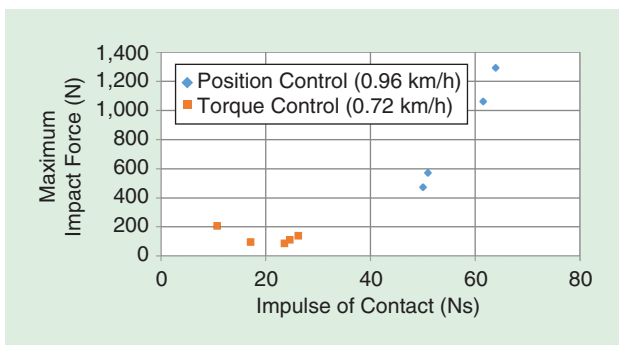


Figure 23. The contact force and impulse in some experiments on the robot's collision at the elbow against an obstacle with the position-based controller (diamond) and the torque-based controller (square).

through a door to enter a room was also realized, as shown in Figure 17(b).

Walking on Scattered Debris

Quadruped walking on scattered debris was tested [Figure 1(c)]. When E2-DR stepped over piled debris on steps (Figure 18), its landing positions were automatically determined according to the surface shape of the measured floors.

Splashproofing

Quadruped walking and climbing up and down a vertical ladder were tested under rain conditions for 20 min, as shown in Figure 19. When the robot was disassembled after the experiments, it was found that a small amount of water had breached the sealed sections due to the weak pressure of the rubber packing.

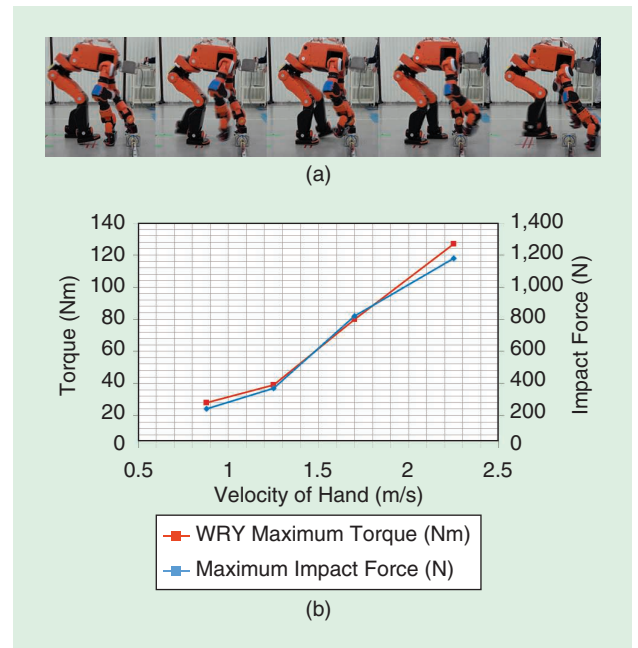


Figure 24. (a) Snapshots of an unexpected collision while walking at 1.44 km/h. (b) The relation between hand velocity and impact force and wrist-pitch joint torque. When the robot moves at 1.44 km/h, the hand velocity is 2.2 m/s. WRY: wrist Y (tilt) joint.

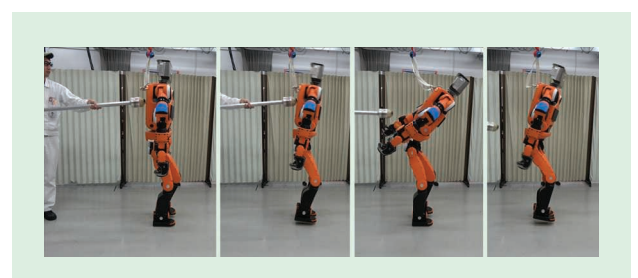


Figure 25. An illustration of E2-DR's push recovery while bipedally stomping. The robot kept its CoM on its supported polygon while absorbing the impact from being pushed.

Additional Movements

Some movements potentially used in actual tasks were also implemented, such as transitioning to a waiting posture and standing up (Figure 20). Although some tests for standing up on debris were successfully accomplished, the level of stability was not sufficient. Here, we have to say that the robot still cannot maintain trouble-free hardware when it falls over.

Experiments to Show the Feasibility to Absorb Collisions

Performance of Whole-Body Movement With a Torque-Based Controller

Experiments on bipedal and quadrupedal walking were conducted. The reference trajectories of these movements were the same as in the experiments with the position-based controller. When the robot speed was more than 1.65 km/h, the tracking error of the CoM became larger, and the robot fell down. Quadruped locomotion over scattered debris was also tested to evaluate E2-DR's robustness against uneven terrain, as shown in Figure 21. In this experiment, the robot assumed that the floor was flat, although the floor was measured previously in the "Walking on Scattered Debris" section. Adaptation to the unevenness of the terrain with the torque-based control was qualitatively faster than with position-based one.

Whole-Body Disturbance Test

The robustness against collision with obstacles and the robot's ability to recover from being pushed were evaluated.

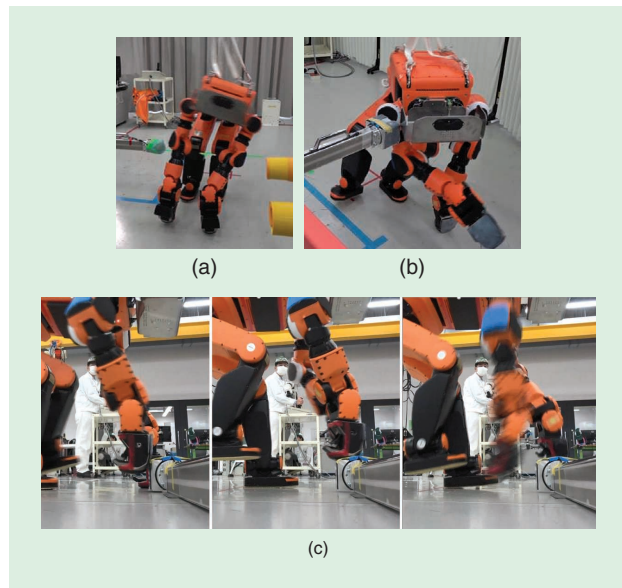


Figure 26. When E2-DR (a) hits its elbow or (b) strikes its shoulder against an obstacle, it sometimes falls down, even if the impact force was well absorbed. (c) In the case where the robot bumps its hand tip against an obstacle on the floor, the hand is placed on the object because of its whole-body compliance. Since the robot does not recognize that its right hand was placed on the obstacle, the robot falls down due to the slipping of its right hand.

Unexpected collisions between an arm and an obstacle while walking were tested, as shown in Figure 22. Experiments were set up so that the elbow or shoulder collided with an obstacle fixed to the floor. The robot stopped just after the impact. Figure 23 shows data on the contact force and impulse during experiments with elbow collision.

E2-DR is a major step

forward as an experimental robot platform to accelerate research toward real-world usage in narrow spaces.

Discussion

The aforementioned experiments show the potential for robots to work in narrow spaces. However, improvements are needed. First, the physical stability is not adequate. In particular, when moving and standing up over scattered obstacles, the robot does not exhibit enough adaptive stability to deal with its unexpected collapse. With regard to the ability to absorb impact from an obstacle, E2-DR is still not sufficiently competent, as demonstrated in Figure 26. In such cases, the robot's posture was largely modified because of the compliance of its whole-body joints. However, the motion controller continued to track the originally planned motion without accounting for the change in posture. Real-time motion planning with whole-body compliance would help solve this issue.

Conclusions

In this article, the new experimental humanoid robot E2-DR, for inspection and disaster response in narrow areas of industrial facilities, was shown. The robot has the following distinctive features:

- adeptness at moving up and down 3D structures
- proficiency in moving in narrow pathways and narrow spaces
- the ability to move over scattered debris
- the capacity to absorb the impact of collisions while moving
- the nature of being dust- and splashproof.

We designed E2-DR to satisfy the requirements for working in narrow areas in industrial plants, but not all of the specifications have been verified up to now. Additionally, not all of the movements could be realized with torque control. Further development is needed to be able to absorb collisions while moving. Unfortunately, there are still big gaps preventing us from using the robot in actual inspections or disaster

responses. However, we think that E2-DR is a major step forward as an experimental robot platform to accelerate research toward real-world usage in narrow spaces.

Acknowledgments

We would like to acknowledge Dr. Shunichi Nozawa, Dr. Youhei Kakiuchi, Prof. Kei Okada, and Prof. Masayuki Inaba of the University of Tokyo for their contributions to the whole-body motion planner in the “Motion Planning” section as a collaboration project. We also gratefully acknowledge the work of past and present members of our laboratory for designing the robot hardware, implementing the software architecture, realizing functions, and conducting experiments. We would also like to thank Chris Garry for his help editing this article.

References

- [1] B. Yamauchi, “Packbot: a versatile platform for military robotics,” in *Proc. SPIE 2004, Unmanned Ground Vehicle Technology VI*, vol. 5422. Orlando, FL: Society of Photo-Optical Instrumentation Engineers, pp. 228–237. doi: /10.1117/12.538328.
- [2] M. Hutter et al., “Anymal: A highly mobile and dynamic quadrupedal robot,” in *Proc. IEEE/RSJ Int. Conf. Intelligent Robots and Systems (IROS)*, 2016, pp. 38–44.
- [3] K. Kojima et al., “Development of life-sized high-power humanoid robot JAXON for real-world use,” in *Proc. IEEE-RAS 15th Int. Conf. Humanoid Robots*, 2015, pp. 838–843.
- [4] M. Zucker et al., “A general purpose system for teleoperation of the DRC HUBO humanoid robot,” *J. Field Robot.*, vol. 32, no. 3, pp. 336–351, 2015.
- [5] P. Hebert et al., “Mobile manipulation and mobility as manipulation: Design and algorithms of RoboSimian,” *J. Field Robot.*, vol. 32, no. 2, pp. 255–274, 2015.
- [6] K. Narukawa, T. Yoshiike, K. Tanaka, and M. Kuroda, “Real-time collision detection based on one class SVM for safe movement of humanoid robot,” in *Proc. IEEE-RAS 17th Int. Conf. Humanoid Robotics*, 2017, pp. 791–796.
- [7] N. A. Radford et al., “Valkyrie: NASA’s first biped humanoid robot,” *J. Field Robot.*, vol. 32, no. 3, pp. 397–419, 2015.
- [8] F. Negrello et al., “WALK-MAN humanoid lower body design optimization for enhanced physical performance,” in *Proc. IEEE Int. Conf. Robotics and Automation*, 2016, pp. 1817–1824.
- [9] T. Yoshiike et al., “Development of experimental legged robot for inspection and disaster response in plants,” in *Proc. IEEE/RSJ Int. Conf. Intelligent Robots and Systems*, 2017, pp. 4869–4876.
- [10] Y. Kanemoto, T. Yoshiike, M. Muromachi, and M. Osada, “Compact and high performance torque-controlled actuators and its implementation to disaster response robot,” in *Proc. IEEE Int. Conf. Robotics and Automation (ICRA)*, 2018, pp. 1–7.
- [11] T. Kamioka, T. Watabe, M. Kanazawa, H. Kaneko, and T. Yoshiike, “Dynamic gait transition between bipedal and quadrupedal locomotion,” in *Proc. IEEE/RSJ Int. Conf. Intelligent Robots and Systems (IROS)*, 2015, pp. 2195–2201.
- [12] N. Paine, J. Holley, G. Johnson, and L. Sentis, “Actuator control for the NASA-JSC Valkyrie humanoid robot: A decoupled dynamics approach for torque control of series elastic robots,” *J. Field Robot.*, vol. 32, no. 3, pp. 378–396, 2014.
- [13] N. G. Tsagarakis, J. Saglia, D. G. Caldwell, and Z. Li, “The design of the lower body of the compliant humanoid robot cCub,” in *Proc. IEEE Int. Conf. Robotics and Automation*, 2011, pp. 2035–2040.
- [14] N. Kashiri, J. Malzahn, and N. G. Tsagarakis, “On the sensor design of torque controlled actuators: A comparison study of strain gauge and encoder-based principles,” *IEEE Robot. Autom. Lett.*, vol. 2, no. 2, pp. 1186–1194, 2017.
- [15] M. Sekiya, N. Neki, Z. Miyashita, and N. Ono, “Development of component based middleware for intelligent robot software,” *Honda R&D Tech. Rev.*, vol. 26, no. 2, pp. 157–164, 2014.
- [16] S. Nozawa, M. Kanazawa, Y. Kakiuchi, K. Okada, T. Yoshiike, and M. Inaba, “Three-dimensional humanoid motion planning using COM feasible region and its application to ladder climbing tasks,” in *Proc. IEEE-RAS 16th Int. Conf. Humanoid Robots*, 2016, pp. 49–56.
- [17] T. Takenaka et al., “Real time motion generation and control for biped robot: 4th report: Integrated balance control,” in *Proc. IEEE/RSJ Int. Conf. Intelligent Robots and Systems*, 2009, pp. 1601–1608.
- [18] M. Kanazawa et al., “Robust vertical ladder climbing and transitioning between ladder and catwalk for humanoid robots,” in *Proc. IEEE/RSJ Int. Conf. Intelligent Robots and Systems (IROS)*, 2015, pp. 2202–2209.
- [19] S. Feng, X. Xinjilefu, C. G. Atkeson, and J. Kim, “Optimization based controller design and implementation for the Atlas robot in the DARPA Robotics Challenge finals,” in *Proc. IEEE-RAS Int. Conf. Humanoid Robots*, 2015, pp. 1028–1035.

Takahide Yoshiike, Honda R&D Co., Ltd., Tokyo. Email: takahide_yoshiike@n.f.rd.honda.co.jp.

Mitsuhide Kuroda, Honda R&D Co., Ltd., Tokyo. Email: mitsuhide_kuroda@n.f.rd.honda.co.jp.

Ryuma Ujino, Honda R&D Co., Ltd., Tokyo. Email: ryuma_ujino@n.f.rd.honda.co.jp.

Yoshiki Kanemoto, Honda R&D Co., Ltd., Tokyo. Email: Yoshiki_Kanemoto@n.f.rd.honda.co.jp.

Hiroyuki Kaneko, Honda R&D Co., Ltd., Tokyo. Email: hiroyuki_kaneko@n.f.rd.honda.co.jp.

Hirofumi Higuchi, Honda R&D Co., Ltd., Tokyo. Email: hirofumi_higuchi@n.f.rd.honda.co.jp.

Satoshi Komuro, Honda R&D Co., Ltd., Tokyo. Email: satoshi_komuro@n.f.rd.honda.co.jp.

Shingo Iwasaki, Honda R&D Co., Ltd., Tokyo. Email: shingo_iwasaki@n.w.rd.honda.co.jp.

Minami Asatani, Honda R&D Co., Ltd., Tokyo. Email: minami_asatani@n.f.rd.honda.co.jp.

Takeshi Koshiishi, Honda R&D Co., Ltd., Tokyo. Email: takeshi_koshiishi@n.w.rd.honda.co.jp.

